CHEMISTRY OF MATERIALS
Article

Chem. Mater. **2010,** *22,* 5949–5956 5949
DOI:10.1021/cm102087e

Carbon Nanotube-Conducting Polymer Core−Shell Hybrid Using an Imidazolium-Salt-Based Ionic Liquid As a Linker: Designed As a Potential Platinum Electrode Alternative Material for Large-Scale Solution Processing

Liping Zhao, Yongjin Li,* Zhifu Liu, and Hiroshi Shimizu

Nanosystem Research Institute, National Institute of Advanced Industrial Science and Technology Tsukuba Central 5, 1-1-1 Higashi, Tsukuba, Ibaraki, 305-8565, Japan

Received July 27, 2010. Revised Manuscript Received September 19, 2010

A core−shell carbon nanotube/conducting polymer hybrid, using an imidazolium-salt-based ionic liquid as a linker, has been developed for large-scale solution processing of CNTs. Dye-sensitized solar cells (DSCs) with the solution processed hybrid film as the counter electrode exhibit comparable photovoltaic performance to that of devices with the conventional Pt counter electrode. A strategy developed is extremely simple and effective with good environmentally compliance. The water-soluble shell (1) promotes dispersion of the CNT aggregates and brings individual CNTs into aqueous solution while maintaining intact π-conjugation structure and (2) leads to a reduced charge injection barrier and realizes high photovoltaic performance. This work paves a way for high-performance optoelectronic and solar energy conversion devices of large-scale applications.

Introduction

The intrinsic mechanical, thermal, and electric properties of carbon nanotubes (CNTs) make them promising components for high-performance devices, including thin-film transistors, solar cells, energy-storage devices, and flexible electronics.[1−8] Successful mass production of CNTs has further accelerated these materials in the large-scale practical applications.[9] To this end, high-volume and low-cost solution processing techniques are highly demanded to produce flexible and homogeneous films over large areas while maintaining the unique properties of CNTs. One of the most critical factors associated with them is the preparation of their stable dispersions, especially CNTs suspensions in water and simple water/organic mixtures with low toxicity and good environmentally compliance. However, the surface of CNTs is rather inert and is generally insoluble in all solvents with surface tensions higher than 100 mN m^{-1}. Therefore, surface modifications by introducing the functional components have been developed to enhance the processability of CNTs.[10−16]

Though covalently functionalized CNTs are easily processed, some of the important properties are lost due to partial destruction of their extended π-conjugation. For example, for each functional group that is added, two π-electrons are removed from the conjugated π system.[10] To keep the electronic properties of CNTs intact, noncovalent modifications of CNTs with appropriate ensembles, such as surfactants and polymers with aromatic functionalities[17,18] and pyrene and its derivatives,[19−21]

*Corresponding author. Telephone: 81-29-861-4197. Fax: +81-29-861-6294. E-mail: yongjin-li@aist.go.jp.

(1) Javey, A.; Guo, J.; Wang, Q.; Lundstrom, M.; Dai, H. J. *Nature* **2003**, *424*, 654–657.
(2) Wu, Z. C.; Chen, Z. H.; Du, X.; Logan, J. M.; Sippel, J.; Nikolou, M.; Kamaras, K.; Reynolds, J. R.; Tanner, D. B.; Hebard, A. F.; Rinzler, A. G. *Science* **2004**, *305*, 1273–1276.
(3) LeMieux, M. C.; Roberts, M.; Barman, S.; Jin, Y. W.; Kim, J. M.; Bao, Z. N. *Science* **2008**, *321*, 101–104.
(4) Itkis, I. E.; Yu, A. P.; Haddon, R. C. *Nano Lett.* **2008**, *8*, 2224–2228.
(5) Fukushima, T.; Aida, T. *Chem.—Eur. J.* **2007**, *13*, 5048–5058.
(6) Nugent, J. M.; Santhanam, K. S. V.; Rubio, A.; Ajayan, P. M. *Nano Lett.* **2001**, *1*, 87–91.
(7) Fan, B. H.; Mei, X. G.; Sun, K.; Ouyang, J. *Appl. Phys. Lett.* **2008**, *93*, 143103 (3 pages) .
(8) Hu, L. B.; Choi, J. W.; Yang, Y.; Jeong, S.; Mantia, F. L.; Cui, L.; Cui, Y. *Proc. Natl. Acad. Sci. U.S.A.* **2009**, *106*, 21490–21494.
(9) Journet, C.; Maser, W. K.; Bernier, P.; Loiseau, A.; Chapelle, M. L.; Lefrant, S.; Deniard, P.; Lee, R.; Fischer, J. E. *Nature* **1997**, *388*, 756–758.
(10) Guldi, D. M.; Taieb, H.; Rahman, G. M. A.; Tagmatarchis, N.; Prato, M. *Adv. Mater.* **2005**, *17*, 871–875.
(11) Liu, J.; Rinzler, A. G.; Dai, H.; Hafner, J. H.; Bradley, R. K.; Boul, P. J.; Lu, A.; Iverson, T.; Shelimov, K.; Huffman, C. B.; Rodriguez-Macias, F.; Shon, Y. S.; Lee, T. R.; Colbert, D. T.; Smalley, R. E. *Science* **1998**, *280*, 1253–1256.
(12) Georgakilas, V.; Tagmatarchis, N.; Pantarotto, D.; Bianco, A.; Briand, J. P.; Prato, M. *Chem. Commun.* **2002**, 3050–3051.
(13) O'Connell, M. J.; Boul, P.; Ericson, L. M.; Huffman, C.; Wang, Y.; Haroz, E.; Kuper, C.; Tour, J.; Ausman, K. D.; Smalley, R. E. *Chem. Phys. Lett.* **2001**, *342*, 265–27.
(14) Zhang, X.; Liu, T.; Sreekumar, T. V.; Kumar, S.; Moore, V. C.; Hauge, R. H.; Smalley, R. E. *Nano Lett.* **2003**, *3*, 1285–1288.
(15) Kim, O. K.; Je, J.; Baldwin, J. W.; Kooi, S.; Pehrsson, P. E.; Buckley, L. J. *J. Am. Chem. Soc.* **2003**, *125*, 4426–4427.
(16) Sinani, V. A.; Gheith, M. K.; Yaroslavov, A. A.; Rakhnyanskaya, A. A.; Sun, K.; Mamedov, A. A.; Wicksted, J. P.; Kotov, N. A. *J. Am. Chem. Soc.* **2005**, *127*, 3463–3472.
(17) Dai, H. *Acc. Chem. Res.* **2002**, *35*, 1035–1044.
(18) Moore, V.; Strano, M.; Haroz, E.; Hauge, R.; Smalley, J. R.; Schmidt, J.; Talmon, Y. *Nano Lett.* **2003**, *3*, 1379–1382.
(19) Gotovac, S.; Honda, H.; Hattori, Y.; Takahashi, K.; kanoh, H.; Kaneko, K. *Nano Lett.* **2007**, *7*, 583–587.
(20) Ehli, C.; Guldi, D. M.; Herranz, M. A.; Martin, N.; Campidelli, S.; Prato, M. *J. Mater. Chem.* **2008**, *18*, 1498–1503.
(21) Pender, B.; Sowards, L.; Hartgerink, J.; Stone, M.; Naik, R. *Nano Lett.* **2006**, *6*, 40–44.

Published on Web 10/07/2010

Scheme 1. Schematic Illustration of Proposed Assembled Structures of IL-MWNT and IL-MWNT/PEDOT:PSS[a]

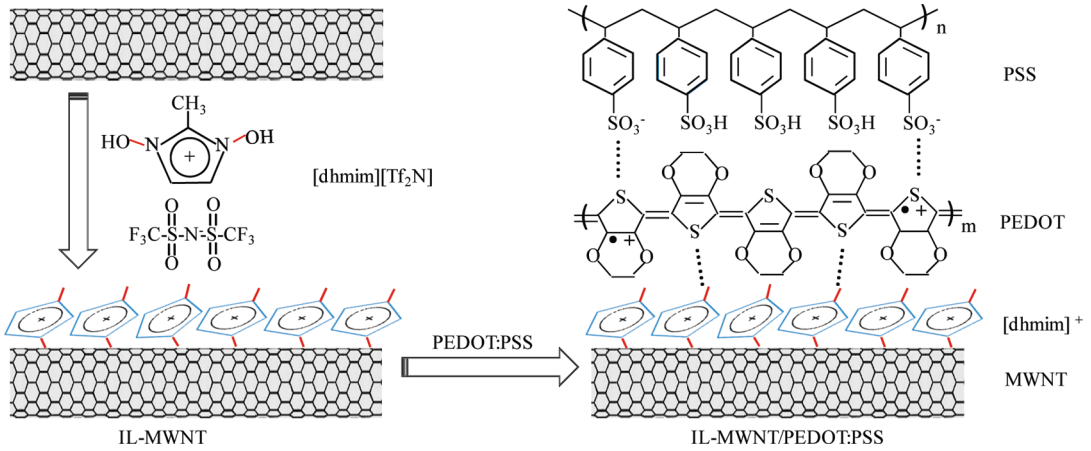

[a] The PEDOT chain in IL-MWNT/PEDOT:PSS exhibits a conductive quinoid structure due to the driving force from the polar hydroxy group interacting with the dipole moment of the ethyldioxythiophene unit on the PEDOT chain. Chemical structures of 1,3-dihydroxy-2-methylimidazolium bis(trifluoromethylsulfonyl)imide ([dhmim][Tf_2N]) and PEDOT:PSS are exhibited.

via $\pi-\pi$ interactions have been achieved for CNT dispersion since they will not induce π-electronic deterioration. For systems where the charge transfer through a CNT scaffold is required, the uses of conductive dispersants are highly desirable for preparing CNT suspensions with satisfactory properties, since the insulating surfactants will limit the charge transfer between the CNTs and their removal is particularly critical. Recently, Aida and co-workers found that CNT bundles can be exfoliated to give finer bundles by imidazolium ionic liquids.[22] As a matter of fact, CNTs noncovalently functionalized with imidazoulium-salt-based ionic liquids could not only preserve the structure intact but also improve the performance of the CNTs.[5] For instance, the application of IL-wrapped CNT bucky gels to electrochemical biosensors, taking advantage of the synergetic catalysis effect between the high electronic conductivity of CNTs and the good ionic conductivity of ILs, can display better performances than CNT-modified electrodes without ILs.[23] ILs wrapped on CNTs can even act as a binder and stabilizer to form CNT/IL/nanoparticles multifunctional hybrids which exhibit good electrocatalytic behaviors.[24,25] However, noncovalent wrapping of CNTs with ILs in practical is not competent to obtain stable dispersions of CNTs either in water or organic solvents. Instead, further study such as polymeric ionic liquids (PIL) and covalently modified with imidazolum ions have been performed for solution processing of CNTs.[5,26]

Here, we present a facile noncovalent association method to obtain stable aqueous dispersions of CNTs inspired by supramolecular concepts. A hydrophilic conductive material poly(3,4-ethylenedioxythiophene): polystyrenesulfonate (PEDOT:PSS) was introduced to form robust interactions of CNTs with ILs as the linker material; the resulting hybrid exhibited a uniform core−shell structure and a good dipersibility in water. Our strategy (Scheme 1) to devise soluble CNT ensembles is realized through a simple two-step procedure. The first step is based on specific interaction between the imidazolium ion component and the π-electronic nanotube surface,[5,22] which results in exfoliated fine nanotube bundles. In the second step, effective interaction of the adsorbed imidazolium ions to PEDOT:PSS finally induces a smooth PEDOT:PSS coating on individually separated CNTs. We have found that 1,3-dihydroxy-2-methylimidazolium bis(trifluoromethylsulfonyl)imide ([dhmim][Tf2N]), an ionic liquid possessing two hydroxy groups (Scheme 1) has a promising efficiency to satisfy the strategy. The multiple polar hydroxy groups readily interact with the PEDOT chains, which are supposed to drive a conformational change and drastically increase the charge-carrier mobility of PEDOT:PSS.[27] This processing method is extremely simple under moderate conditions and utilizes inexpensive aqueous-based techniques; consequently, it can readily be scaled up. In particular, it is not accompanied by the disruption of the π-conjugated nanotube structure and thus maintains intact electric properties. Furthermore, because ionic liquids are ion conductive, their composites are expected to be promising components for electrochemical devices, such as solar cells.[5] Notably, we demonstrate that dye-sensitized solar cells (DSCs) with solution processing of the core−shell IL-MWNT/PEDOT:PSS composite film as the counter electrode exhibit high photovoltaic performance, close to that of devices with the conventional Pt counter electrode and significantly higher than for devices with composite film of pristine MWNT directly mixed with PEDOT:PSS as the counter electrode. The high photovoltaic performances benefit from the high-quality

(22) Fukushima, T.; Kosaka, A.; Ishimura, Y.; Yamamoto, T.; Takigawa, T.; Ishii, N.; Aida, T. *Science* **2003**, *300*, 2072–2074.
(23) Liu, Y.; Zou, X.; Dong, S. *Electrochem. Commun.* **2006**, *8*, 1429–1434.
(24) Wu, B.; Hu, D.; Kuang, Y.; Liu, B.; Zhang, X.; Chen, J. *Angew. Chem., Int. Ed.* **2009**, *48*, 4751–4754.
(25) Guo, S.; Dong, S.; Wang, E. *Adv. Mater.* **2010**, *22*, 1269–1272.
(26) Marcilla, R.; Curri, M. L.; Cozzoli, P. D.; Martinez, M. T.; Loinaz, I.; Grande, H.; Pomposo, J. A.; Mecerreyes, D. *Small* **2006**, *2*, 507–512.
(27) Ouyang, J.; Chu, C.; Chen, F.; Xu, Q.; Yang, Y. *Adv. Funct. Mater.* **2005**, *15*, 203–208.

CNT film with high electrical conductivity and large surface area. CNTs are homogeneously distributed in the film and exhibit high charge exchange currents. Moreover, the new CNT hybrid system with a uniform PEDOT:PSS shell will be of great value for taking advantage of its versatility with respect to ease of dispersion and the prominent applications for PEDOT as well. Driven by the unique electrochemical and spectroscopic properties,[27,28] PEDOT and derivatives have been applied in wide-ranging applications, from electrode materials to biosensors and other applications using biological media. For example, Abidian and co-workers have reported that PEDOT nanotubes could improve the long-term function of neural microelectrodes and the use of PEDOT nanotubes for highly selective, chronic neural recordings at the microscale.[29,30]

Experimental Section

In total, 10 mg of MWNTs (Nikkiso Co. Ltd.) and 1,3-dihydroxy-2-methylimidazolium bis(trifluoromethylsulfonyl)-imide ([dhmim][Tf2N], Aldrich) were mixed and kneaded with an agate mortar in 1:1 weight ratio at room temperature for 30 min. The mixture was washed with ethanol to remove nonadsorbed ionic liquid. After centrifugation, the residue (denoted IL-MWNT) was added to 20 mL of PEDOT:PSS aqueous solution (Aldrich, 1.3 wt %, conductivity 1 S cm^{-1}), which was diluted to 0.05 wt % in water and the mixture sonicated in a low power ultrasonic bath for 10 min. This resulting stable dispersion was centrifuged and then thoroughly washed with water to remove unbonded polymer. The final product was denoted as IL-MWNT/PEDOT:PSS. A reference sample was prepared by directly mixing MWNTs with PEDOT:PSS solution (0.05 wt %) and sonicating the mixture with a probe sonicator (Branson Digital Sonifier 2500 A) for 15 min. The dispersed solid was thoroughly washed with water to remove unbonded polymer, and the final product was denoted as I-MWNT/PEDOT:PSS. No dispersion of MWNTs was observed if the mixture was sonicated with a low-power ultrasonic bath even for over 10 h.

TEM images were recorded with a high acceleration voltage transmission electron microscope (TECNAI G2-F20; FEI Co.). Typically, we cast one drop of dilute aqueous solution onto a 3 mm, 200 mesh copper grid for each of three samples. TGA analysis was carried out using a TG/DTA 7200 (SII Nanotech Inc.) instrument. The samples were dried at 60 °C overnight in vacuum before measurements were performed. Raman spectra were recorded with a Raman system (JASCO NRS-2100) with a 514.5 nm Ar laser as the excitation source.

A simple solution-cast approach was employed to deposit counter electrode materials onto fluorine-doped tin oxide (FTO, Asahi Technoglass) glass substrates. After dropping composite aqueous solutions on FTO substrates, the composite films were dried at 60 °C on a hot plate and annealed at 200 °C overnight. The thickness of the composite film was controlled upon adjusting the weight content of MWNTs. A typical MWNTs concentration of the deposited films was 0.5 mg cm^{-2}. A Pt counter electrode was prepared by magnetron sputtering onto the FTO glass substrate. A PEDOT:PSS counter electrode was prepared by directly dropping 0.5 mL PEDOT:PSS solution (1.3 wt %) onto FTO glass substrate, drying at 60 °C on a hot plate, and annealing at 200 °C overnight. The working electrode was made of commercial TiO_2 paste (Degussa P25) on FTO glass substrate, annealed at 500 °C for 1 h. The sintered TiO_2 film was immersed in 0.5 mmol L^{-1} N719 dye (Solaronix SA, Switzerland) solution in 1:1 acetonitrile and *tert*-butanol. The sensitized photoanodes were removed after 12 h and washed with ethanol before blowing dry with nitrogen. All FTO glass substrates used to make electrodes were made with the same size (15 mm × 15 mm). For photoelectrochemical measurements, the N719 dye sensitized photoanodes were sealed in sandwich cells with a 30 μm spacer by using prepared counter electrodes. The redox electrolyte used was 0.1 M LiI, 0.05 M I_2, 0.6 M dimethyl propyl imidazolium iodide, and 0.5 M *tert*-butylpyridine in dried acetonitrile.

The photovoltaic performance of the assembled solar cells was measured with a source meter (Advantest, R6246), employing an AM 1.5 solar simulator (Wacom Co.,WXS-80C3 with a 300 W Xe lamp and an AM filter) as the light source. The incident light intensity was calibrated using a standard solar cell composed of a crystalline silicon solar cell and an IR-cut off filter (Schott, KG-5), giving the photoresponse range of an amorphous silicon solar cell (produced and calibrated by the Japan Quality Assurance Organization). To avoid the penetration of diffuse light into the active dye-sensitized film, a black mask with an aperture area of 0.2354 cm^2 was employed to measure the photovoltaic performance.

The monochromatic incident photon to current conversion efficiency (IPCE) of the solar cells was measured with a SM-250DAM system (Bunkoh-Keiki Co., Ltd.). The photovoltaic performance of the solar cells was measured with a source meter (Keithley 2400), employing an AM 1.5 solar simulator (Peccell Technologies, Inc., PEC-L11) as the light source. The incident light intensity was calibrated using a standard crystalline silicon solar cell (produced and calibrated by the Japan Quality Assurance Organization).

Results and Discussion

A mixture of MWNTs and [dhmim][Tf2N] was kneaded with an agate mortar in a 1:1 weight ratio at room temperature and formed a gelatinous composite material (this ionic liquid [dhmim][Tf2N] treated MWNT is denoted by IL-MWNT). Heavily entangled carbon nanotube bundles were thought to be exfoliated within the gel to form physical cross-linking of finer bundles mediated by local molecular ordering of the ionic liquids.[22] It is worthy of note that although [dhmim][Tf2N] is solid at room temperature and exhibits a melting point at 72 °C, a physical gel can form at room temperature. The fine structures of the as-prepared IL-MWNT nanocomposites were investigated by transmission electron microscopy (TEM). IL-MWNTs were revealed as fine bundles of several nanotubes and individually separated nanotubes, which confirmed the debundling of the CNTs (Figure S1 in the Supporting Information). That is, the nanotubes did not assemble into tangled ropes after functionalization of the surface with the ionic liquid [dhmim][Tf2N]. On the basis of studies of ionic liquids gel with carbon nanotubes,[5] the polar imidazolium ions around the MWNTs decreased

(28) Groenendaal, L. B.; Jonas, F.; Freitag, D.; Pielartzik, H.; Reynolds, J. R. *Adv. Mater.* **2000**, *12*, 481–494.
(29) Abidian, M. R.; Corey, J. M.; Kipke, D. R.; Martin, D. C. *Small* **2009**, *6*, 421–429.
(30) Abidian, M. R.; Ludwig, K. A.; Marzullo, T. C.; Martin, D. C.; Kipke, D. R. *Adv. Mater.* **2009**, *21*, 3764–3770.

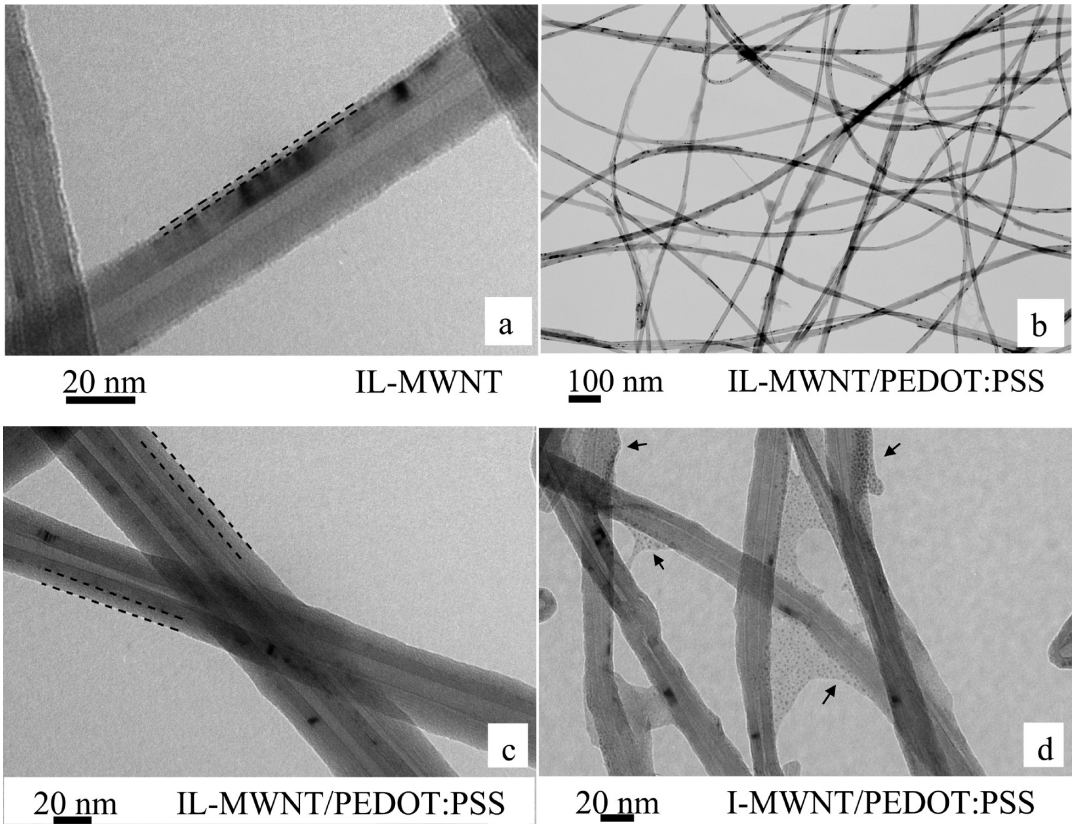

Figure 1. Representative TEM micrographs of (a) IL-MWNT; (b, c) IL-MWNT/PEDOT:PSS at two magnifications (the dotted lines have been added as a visual guide to the coating layers); and (d) I-MWNT/PEDOT:PSS; the arrows have been added to indicate the tiny PEDOT particles on the nanotube surface.

the intrinsic van der Waals forces of the nanotubes, consequently the nanotubes were well dispersed. Furthermore, a very thin coating layer of ionic liquid molecules, typically with 2−3 nm uniform thickness, was observed on the outer surface of the carbon nanotubes (Figure 1a). The imidazolium ions could be adsorbed due to so-called cation−π and/or $\pi-\pi$ interaction between the imidazolium ion and the π-electronic nanotube surface. The $[dhmim]^+$ and $Tf2N^-$ moieties no longer form a hydrogen-bonded pair; the $dhmim^+$ moiety leaves $Tf2N^-$ and sticks to the nanotube surface (Scheme 1). Calculated with a bilayer interspacing of 0.46 nm between adsorbed imidazolium ions, it is a coating compromising about 5 or 6 layers of $[dhmim]^+$ ions.[5]

The nanotube surface with adsorbed $[dhmim]^+$ cations allows further incorporation. Because of the possible electrostatic interaction between imidazolium ions and PSS^- chains and also the interaction between hydroxy groups and PEDOT chains, PEDOT:PSS is attracted to the MWNT surface in which IL-MWNT may acts as a linear template for the linear conformation of PEDOT:PSS and makes the backbone chains pack more efficiently (Scheme 1, IL-MWNT/PEDOT:PSS denotes the hybrid of IL-MWNT and PEDOT:PSS). This interaction can occur readily in aqueous solution under moderate conditions, resulting in a core−shell structure of a uniform layer of organic materials wrapped around MWNT. Typically, an aqueous solution of the ionic liquid modified MWNTs (IL-MWNTs) was ultrasonicated for 10 min in the presence of excess PEDOT:PSS. The solid product was collected by centrifugation and thoroughly washed with water. TEM images (Figure 1b,c and Figure S2 in the Supporting Information) confirmed that the derivatives were composed of highly untangled small bundles of MWNTs and individually distributed MWNTs, with very long MWNTs up to several tens of micrometers in length. Moreover, by decoration of the sidewalls of individual MWNTs with $[dhmim]^+$ and PEDOT:PSS, a core−shell structure with MWNTs at the center can be clearly observed for the nanocomposites. The individual IL-MWNT/PDEOT:PSS nanotube appears to have uniform diameter along their lengths with smooth coverage of the MWNT, supporting the interpretation that the organic molecules are uniformly wrapped around the tubes rather than associated with the side walls at various points as random coils. Such a core−shell structure can be called a molecular nanocomposite because of a robust linkage between the core and the shell. Estimation from TEM images suggests that the average thickness is approximately 8 nm. We believe that the difference of the thickness between IL-MWNT and IL-MWNT/PEDOT:PSS, 2−3 and 8 nm respectively, indicates the existence of a 5−6 nm thick PEDOT:PSS shell. The processing of MWNT with [dhmim][Tf2N] provides facile fabrication of a novel hybrid of MWNT and conducting polymer PEDOT:PSS with a core−shell structure. The smooth PEDOT:PSS shell is thought to be an expanded coil or linear conformation induced by polar

Scheme 2. (a) Schematic Structure of PEDOT:PSS Where the PEDOT Chain Has Coil Conformation; (b) the Benzoid Structure of Thiophene Rings on the PEDOT Chain in the Coil Conformation; (c) Schematic Structure of PEDOT:PSS Where the PEDOT Chain Has a Linear Conformation, and (d) the Quinoid Structure of Thiophene Rings on the PEDOT Chain in the Linear Conformation

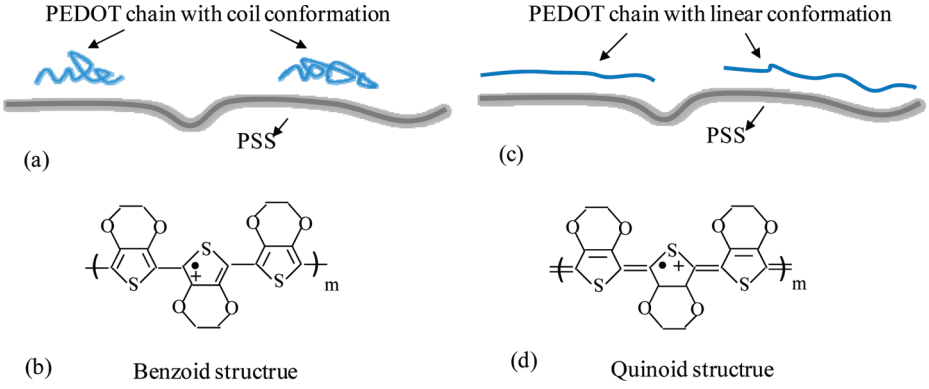

hydroxy groups, which is the conformation that exhibits high charge-carrier mobility (Scheme 2).[27] Furthermore, with benefit from the advantages of processing carbon nanotubes with ionic liquids, it avoids the major problem of π-electronic deterioration and can readily be scaled up.[5]

This novel IL-MWNT/PEDOT:PSS hybrid shows much higher solubility and better dispersibility, compared with pristine MWNTs. As PEDOT:PSS is highly polar, the IL-MWNT/PEDOT:PSS hybrid materials were readily dispersed in water and polar organic solvents such as dimethyl sulfoxide (DMSO) and *N*,*N*-dimethylformamide (DMF). The polymer and CNT comprise a single entity that can be manipulated as a whole, rather than by solubilization via a dynamic equilibrium of supramolecular association. We have confirmed that this IL-MWNT/PEDOT:PSS is uniformly dispersed in commercial PEDOT:PSS solution to form homogeneous suspensions, and SEM images (Figure S3 in the Supporting Information) of the spin-coated composite film revealed individually separated carbon nanotubes distributed in the PEDOT:PSS matrix. We have also established that this processing procedure can be applied to single-walled carbon nanotubes (SWNTs) as well (Figure S4 in the Supporting Information). Details of this work will be reported in the near future.

By contrast, a composite of MWNT/PEDOT:PSS with pristine MWNTs (denoted I-MWNT/PEDOT:PSS) exhibited a noncontinuous layer and much increased roughness resulting from random wrapping of PEDOT:PSS on the nanotube surface (Figure 1d), even under high power ultrasonication. Because of $\pi-\pi$ coupling and/or hydrophobic interaction between conductive PEDOT and the π-electronic nanotube surface, an uneven 2 nm coating of PEDOT:PSS molecules was obtained. This thickness is consistent with that of ionic liquid $[dhmim]^+$ ions adsorbed on the nanotube surface through $\pi-\pi$ and/or cation$-\pi$ coupling and may be the limiting distance to effect noncovalent physical stacking interactions. Instead of the uniform smooth surface of the IL-MWNT/PEDOT:PSS hybrid, tiny particles and amorphous polymer agglomerations were commonly observed within the I-MWNT/PEDOT:PSS hybrid material; the tiny particles are suggested to be the coil conformation of PEDOT

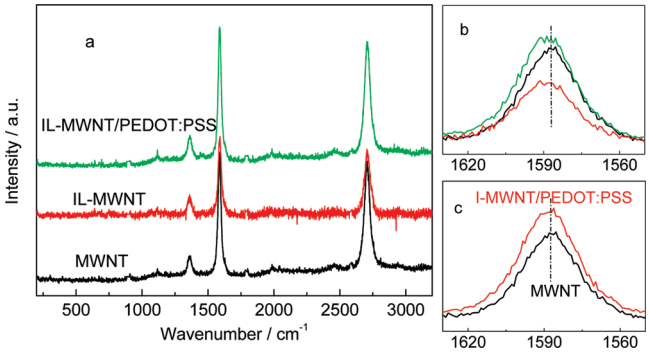

Figure 2. (a, b) Raman spectra of MWNT, IL-MWNT, and IL-MWNT/PEDOT:PSS at (a) 200−3200 cm^{-1} and (b) 1550−1630 cm^{-1} and (c) Raman spectra of MWNT and I-MWNT/PEDOT:PSS at 1550−1630 cm^{-1}.

chains (Scheme 2). In the absence of ionic liquid molecules, it is difficult or even impossible to induce the change from coil to linear conformation and both coil and linear structures of the PEDOT chains exist in the PEDOT:PSS molecules around the MWNTs. Although the IL-MWNT/PEDOT:PSS hybrid has random wrapping of PEDOT:PSS on the MWNT surface, it gives better dispersibility than pristine MWNTs and in additional results of separated fine bundles of MWNTs.

Raman spectroscopy is a useful tool for the characterization of functionalized carbon nanotubes. As shown in Figure 2a (514.5 nm excitation), the D- and G-bands of MWNTs, attributed to the defects/disorder-induced and in-plane vibration modes, respectively, are clearly observed for pristine MWNTs and functionalized MWNTs. All Raman spectra have the same pattern and D- to G-band intensity ratios exhibited minimal values, which imply that the solubilization procedure did not affect the graphite structure of the MWNTs. In contrast to pristine MWNTs, a shift to higher wavenumber of the tangential G-band was observed for functionalized MWNTs composites (Figure 2b): the bands appear at 1587.5, 1589.3, and 1589 cm^{-1} for pristine MWNTs, IL-MWNTs, and IL-MWNTs/PEDOT:PSS, respectively. Moreover, the Raman peak intensities of all bands for IL-MWNTs are obviously lower than those of the corresponding bands for the pristine MWNTs. After interacting with

PEDOT:PSS molecules, the Raman signals of IL-MWNTs/PEDOT:PSS were enhanced and even stronger than the corresponding bands for the pristine MWNTs. A similar Raman signal enhancement has been reported for PAA-coated CNTs.[31] Although the reason is not clear at this moment, a provisional mechanism was proposed. The Raman signal difference suggests strong interactions of IL on the MWNTs surface and PEDOT:PSS on the IL-MWNTs surface, which induces energy transfer between CNTs and coating molecules and subsequently affects the electronic properties of CNTs. The G-band is known to be associated with carbon atom vibrations along the nanotube axis. It has been reported that the Raman frequency of the G-band is sensitive to charge transfer from dopant additions to SWNTs: upshifts for acceptors and downshifts for donors.[32] Within IL-MWNT, the so-called "cation$-\pi$" and/or $\pi-\pi$ interactions between the $[dhmim]^+$ ions and the π-electronic nanotube surface affects the electron density and increases the energy necessary for carbon atom vibrations to occur, which is reflected in the higher frequency of Raman peaks.[15,31] Although it was reported that the adsorption of ionic liquid molecules on CNT is due to weak van der Waals interactions,[33] shift and peak intensity change of the G band demonstrate the fact that the electronic structure changes of CNTs and favors strong cation$-\pi$ or $\pi-\pi$ interactions. In addition, both obvious shift and intensity change of the G band and RBM were observed on Raman spectra of the SWNT/ionic liquid hybrid during our study (not presented), which confirmed charge transfer and the electronic structure change as well. Another explanation for the observed upshifts of the G-band frequencies is an increase in the elastic constant of the harmonic oscillator due to the mechanical confinement produced by the strong coating of organic molecules on the nanotube surface. In the case of I-MWNT/PEDOT:PSS (Figure 2c), the Raman shift of the G-band is 1588 cm^{-1}, which is 0.5 cm^{-1} upshifted compared with that of pristine MWNTs or simply caused by the instrument resolution deviation. The weak effects of PEDOT:PSS on the Raman signal of MWNTs, corresponding to weak interaction between PEDOT:PSS and pristine MWNTs, contrasts with the interactions in IL-MWNTs and IL-MWNT/PEDOT:PSS.

DSCs have attracted considerable attention as one of the new generation of low-cost, high-efficiency, environment-friendly photovoltaic systems. Improving the performance of both the photoanode and counter-electrode to achieve maximum efficiency, and development of low cost materials, are important strategies to realize the commercial potential of DSCs. The efficiencies of DSCs using the IL-MWNT/PEDOT:PSS core$-$shell hybrid film as counter electrodes, which were prepared by a simple solution-cast approach, were determined.

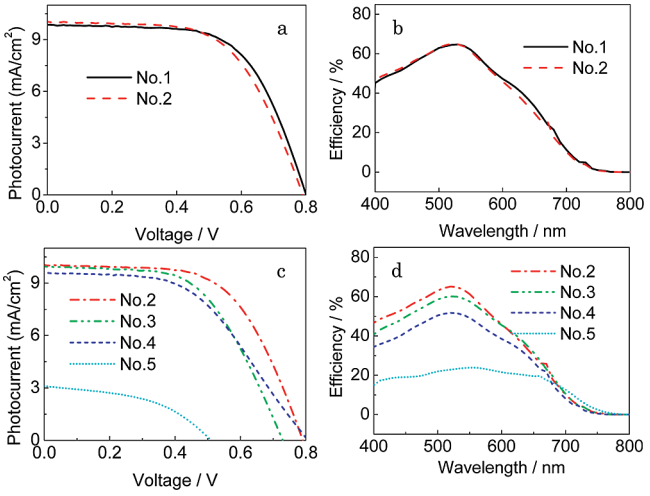

Figure 3. (a, c) Photocurrent$-$photovoltage characteristics and (b, d) monochromatic IPCE spectra of the DSCs with Pt (no. 1); IL-MWNT/PEDOT:PSS (no. 2); I-MWNT/PEDOT:PSS (no. 3); IL-MWNT (no. 4); and PEDOT:PSS (no. 5) films as counter electrodes.

Current$-$voltage ($I-V$) curves of the DSCs with different counter electrodes are shown in Figure 3a,c. The $I-V$ curve of a DSC using Pt as the counter electrode is included for comparison. The photovoltaic parameters of these devices, including the short-circuit current (J_{sc}), the open-circuit voltage (V_{oc}), the fill factor (FF), and the energy conversion efficiency (η), are summarized in Table 1. As expected due to the low conductivity of the PEDOT:PSS layer, a PEDOT:PSS counter-electrode based DSC device showed extremely poor photovoltaic performance with J_{sc} = 3.31 mA cm^{-2}, V_{oc} = 0.52 V, FF = 0.50, and η = 0.88%. Despite IL-MWNTs and I-MWNT/PEDOT:PSS films showing exfoliated fine bundles with large specific surface area, both counter electrodes exhibited poor FF and hence η, which can be attributed to limited charge-carrier mobility of the coverage layers. The charge transfer process contributes to the internal series resistance, which affects only FF to some extent and all MWNT-based devices exhibit, accordingly, similar values of J_{sc} and V_{oc}. In sharp contrast, the DSC with the IL-MWNT/PEDOT:PSS film as the counter electrode exhibited high photovoltaic performance: J_{sc} = 9.95 mA cm^{-2}, V_{oc} = 0.79 V, FF = 0.60, and η = 4.77%. This performance matched that of the DSC with a Pt counter electrode and is significantly higher than for the I-MWNT/PEDOT:PSS counter electrode. These results demonstrate a promising candidate to replace the high cost Pt with the cost-effective hybrid materials as counter electrodes of DSCs.

Incident photon to current conversion efficiency (IPCE) spectra (Figure 3b,d) of the DSCs exhibit good consistency with the $I-V$ curves. Maximum IPCE of 64.7, 64.8, 60, and 51.5% at 530 nm was observed for DSCs with Pt, IL-MWNTs/PEDOT:PSS, I-MWNTs/PEDOT:PSS, and IL-MWNTs films, respectively, as counter electrodes. The IPCE spectrum of the DSC with the PEDOT:PSS film as the counter electrode showed much lower IPCE of 23% at 530 nm for the same electrolyte.

(31) Liu, A.; Honma, I.; Ichihara, M.; Zhou, H. *Nanotechnology* **2006**, *17*, 2845–2849.
(32) Dresselhaus, M. S.; Dresselhaus, G.; Saito, R.; Jorio, A. *Phys. Rep.* **2005**, *409*, 47–99.
(33) Wang, J.; Chu, H.; Li, Y. *ACS Nano* **2008**, *2*, 2540–2546.

Table 1. Photovoltaic Performance Parameters of DSCs with Pt, IL-MWNTs/PEDOT:PSS, I-MWNTs/PEDOT:PSS, and IL-MWNTs Films As Counter Electrodes

sample	Pt	IL-MWNT/PEDOT:PSS	I-MWNT/PEDOT:PSS	IL-MWNT	PEDOT:PSS
J_{sc}/mA cm^{-2}	9.89	9.95	9.9	9.50	3.31
V_{oc}/V	0.80	0.79	0.73	0.80	0.52
FF	0.62	0.60	0.57	0.50	0.50
η (%)	4.94	4.77	4.12	3.80	0.88

Since both IL-MWNT/PEDOT:PSS and I-MWNT/PEDOT:PSS films are well dispersed nanotube networks with large surface areas which can serve as conductive pathways from the electrodes, we speculate that their different photovoltaic performances were due to the difference of charge-carrier mobility resulting from the conformational change of the PEDOT chains within the two hybrid systems. Coil and linear or expanded-coil conformations have been proposed for the PEDOT chains in conducting polymer PEDOT:PSS.[34] In the coil conformation, the plane of a thiophene ring on the PEDOT chain deviates greatly from the plane of its neighboring thiophene ring, so that the $C_\alpha-C_\alpha$ bond between the two thiophene rings is more like a σ bond and has a low charge-carrier mobility. However, in an expanded-coil or linear conformation, the neighboring thiophene rings in the PEDOT chains are oriented almost in the same plane so that the conjugated π-electrons can be delocalized over the whole chain. That is to say, the benzoid structure is the favored structure for a coil conformation, while the quinoid structure is favored for a linear or expanded-coil conformation. Thus, it is understandable that the PEDOT:PSS chains with expanded-coil or linear conformations have high charge-carrier mobility and stronger interchain interactions among the PEDOT chains than is the case for PEDOT chains in the coil conformation (Scheme 2).

For the IL-MWNT/PEDOT:PSS hybrid system, the adsorbed $[dhmim]^+$ is an imidazolium ion component possessing two hydroxy groups, which is similar to polyalcohols. A common feature of polyalcohol doping is that one hydroxy group forms a hydrogen bond to the sulfonate or sulfonic acid group of PSS, while the dipole of another hydroxy group interacting to the dipole moment or the positive charge of the thiophene unit on the PEDOT chains.[27] It is claimed that this dipole−dipole or dipole−charge interaction is effective for the quinoid conformational change of the thiophene rings of the PEDOT segments.[27] In the case of $[dhmim]^+$, in addition to interaction of hydroxy group and sulfonate/sulfonic acid group, a strong electrostatic interaction must exist between imidazolium ions and PSS^- chains. Those interactions reduce the distance between the hydroxy groups in the $[dhmim]^+$ component and the thiophene rings of PEDOT, which is close enough to promote effective dipole−dipole or dipole−charge interactions. All of the above interactions between the adsorbed $[dhmim]^+$ ions on the nanotube surface and the PEDOT segments favor a conformational change of the PEDOT chain from coil to linear or expanded-coil structure, and the linear or expanded-coil structure becomes dominant in the PEDOT:PSS layer on the IL-MWNT surface. Furthermore, the contribution of dipole−dipole or dipole−charge interactions decreases the potential barrier for carrier transport between the ionically conducting imidazolium component and PEDOT oligomers. This highly conductive PEDOT:PSS wrapping on the IL-MWNT does not affect the carrier transfer, since the carrier can transport from IL-MWNT to PEDOT and carrier transfer can take place on PEDOT as well (Scheme 3). For the I-MWNT/PEDOT:PSS hybrid system, however, both benzoid and quinoid resonant structures of the thiophene ring exist on the PEDOT:PSS chains, which finally results in lower charge-carrier mobility compared with IL-MWNT/PEDOT:PSS nanocomposites.

Scheme 3. Schematic Electron Path of DSCs with IL-MWNT/PEDOT:PSS Film As Counter Electrode, Where the Electron Can Transport from PEDOT to IL-MWNT and Can Take Place on PEDOT As Well[a]

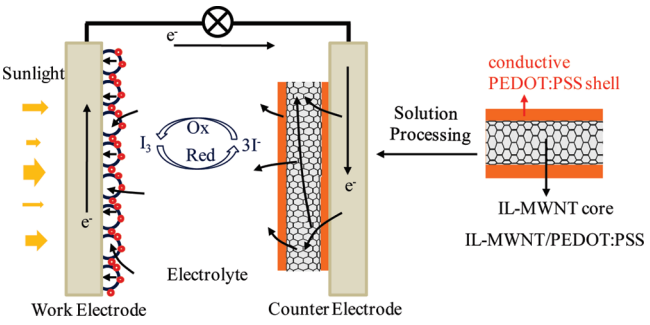

[a] The conductive shells of PEDOT:PSS molecules are active catalysts for reduction of I_3^-.

We also observed that the annealing temperature of the IL-MWNT/PEDOT:PSS film strongly affected both the photovoltaic performance and $I-V$ plots (Figure S5 in the Supporting Information) of the DSCs. The photoconversion efficiency increased for the device with the films aged at a higher temperature as the counter-electrode. This effect can most likely be attributed to the decomposition of PEDOT:PSS at high temperature: thermal aging induces hole polarons on the PEDOT oligomers to wander further from the polaron vicinity and increase the mobility of the hole carriers.[35] Moreover, the bonds between PEDOT and PSS may break during thermal treatment, especially with the existence of competitive electrostatic interaction from cation $[dhmim]^+$ to PSS, which further reduces the rupture energy of the electrostatic bonding between PSS and PEDOT. The PSS chains bearing negative charge repel each other resulting

(34) Bagchi, D.; Menon, R. *Chem. Phys. Lett.* **2006**, *425*, 114–117.

(35) Vitoratos, E.; Sakkopoulos, S.; Dalas, E.; Paliatsas, N.; Karageorgopoulos, D.; Petraki, F.; Kennou, S.; Choulis, S. A. *Org. Electron.* **2009**, *10*, 61–66.

in better alignment of those chains and leave the conductive PEDOT segments concentrated between them, further enhancing the mobility of the hole polarons in the PEDOT oligomers. However, the mechanism of the enhancement of photovoltaic performance of the IL-MWNT/PEDOT:PSS hybrid film during heat annealing is still an assumption and needs further study.

Conclusions

In summary, the high conductivity IL-MWNTs/PEDOT:PSS hybrid has been developed with a novel core−shell structure. With the benefits from the advantages of processing carbon nanotubes with ionic liquids, it (1) is readily obtained through a simple two-step procedure under moderate conditions; (2) does not disrupt the extended π networks; (3) exhibits stable and robust interactions to form a uniform conductive layer; and (4) exhibits high charge-carrier mobility. The conducting polymer and CNT comprise a single entity that can be manipulated as a whole with high solubility and good dispersibility in water, rather than by solubilization via a dynamic equilibrium of supramolecular association. The composite films can be deposited on various substrates using inexpensive low-temperature deposition techniques, which is a facile and practical processing method that allows for large-scale processing of CNTs. The high photovoltaic performance expands the scope of low-cost, high-efficiency DSCs for practical applications. Indeed, its simple organizational principles open a new avenue in the design of large size optoelectronic and solar energy conversion devices, including flexible electronics.

Acknowledgment. This work was partially supported by a Grant-in-Aid for Scientific Research from the Japan Society for the Promotion of Science (Grant 21760543). The authors would like to acknowledge Dr. M. Miyauchi for experimental support to test the photovoltaic performance and the monochromatic IPCE of the assembled solar cells.

Supporting Information Available: TEM images of IL-MWNT and IL-MWNT/PEDOT:PSS indicating a thick bundle of MWNTs debundling to form thinner bundles and individual nanotubes with surface functionalization, SEM image of the cross-section of the PEDOT:PSS composite film with IL-MWNT/PEDOT:PSS and IL-SWNT/PEDOT:PSS, and photocurrent−photovoltage characteristics of DSCs with various thermally treated IL-MWNT/PEDOT:PSS films as counter electrodes exhibiting temperature dependent tendencies (PDF). This material is available free of charge via the Internet at http://pubs.acs.org.